QUANTUM MOLECULAR DYNAMICS SIMULATIONS OF PROCESSES IN LARGE CLUSTERS: METHODS AND APPLICATIONS

R.B. GERBER,[(a),(b)] P. JUNGWIRTH,[(c)] E. FREDJ,[(a)]
and A.Y. ROM[(b)]

[(a)] *Department of Physical Chemistry*
and The Fritz Haber Research Center,
The Hebrew University, Jerusalem 91904, Israel

[(b)] *Department of Chemistry*
University of California,
Irvine, CA 92697-2025, U.S.A.

[(c)] *J. Heyrovsky Institute of Physical Chemistry*
Academy of Sciences of the Czech Republic
Dolejskova 3, 18223 Prague 8, Czech Republic

Abstract

Methods for time-dependent quantum-mechanical simulations of large polyatomic systems are described and analyzed, and applications to processes in clusters are presented. Two basic methods are discussed: (i) The Time-Dependent Self-Consistent Field (TDSCF) approximation and its generalizations; (ii) The Classically-Based Separable Potential (CSP) approach, and its extensions. At their simplest respective levels, both methods assume separability of the different modes of the system, and describe each mode as moving in a mean field due to the other modes. In TDSCF the effective single-mode potentials are computed quantum-mechanically, in CSP they are obtained from a classical MD simulation that precedes the quantum calculation. For both methods, improvements are available that correct for correlations between different modes, resulting in approaches of good accuracy. Both the TDSCF and the CSP approach make possible calculations for systems of size and complexity that could hitherto not be treated. Algorithmic and computational aspects of the two methods are examined, and it is found that in typical molecular applications the methods are nearly identical in accuracy, but CSP is greatly superior computationally, especially in applicability to much larger systems than TDSCF. Applications of the methods are presented for: (1) Photoexcitation dynamics and spectroscopy of atomic and molecular impurities in large clusters, e.g., for $I_2(Ar)_n$. (2) Collision dynamics, energy transfer and state-to-state transitions in atom-cluster scattering,

e.g., $He + (Ar)_n, Ar + (H_2O)_n$. Future research directions are suggested in the light of the algorithmic aspects and the applications.

1 Introduction

Quantitative quantum-mechanical calculations are the preferable, rigorous theoretical approach to dynamical processes in systems of a few atoms. There is a large arsenal of powerful, well established methods for quantum-mechanical computations of processes such as photoexcitation, photodissociation, inelastic scattering and reactive collisions for systems having, in the present state-of-the-art, up to three or four atoms, typically.[1–9] Both time-dependent and time-independent "numerically exact" algorithms are available for many of the processes, so in cases where potential surfaces of good accuracy are available, excellent quantitative agreement with experiment is generally obtained. In addition to the full quantum-mechanical methods, sophisticated semiclassical approximations have been developed that for many cases are essentially of near-quantitative accuracy and certainly at a level sufficient for the interpretation of most experiments.[10–13] These methods also are computationally applicable in the present state-of-the-art, to systems of several atoms only.

The situation for large polyatomic systems, as well as for condensed phases is very different. Quantum-mechanical simulation methods of quantitative accuracy have not been available for dynamical processes in systems of many coupled degrees of freedom. Classical Molecular Dynamics (MD) simulations have been the prime theoretical tool for interpretation, analysis and comparison with experiment. They are computationally feasible in the present state-of-the-art for systems having up to tens of thousands of atoms, and have been extensively applied to processes in biomolecules, large molecular aggregates and condensed phases. However, many physical properties cannot be treated classically, at least not quantitatively. Resonance Raman spectroscopic intensities in condensed phases, and state-to-state transitions in atom scattering from large molecules are only two examples in a virtually endless list of observable properties for which classical calculations are not adequate.[14] To this one must add the need to describe quantum effects such as zero-point motions, nonadiabatic transitions and tunneling events in the dynamics of many large systems. The need for a quantitative quantum-mechanical description of large polyatomic systems is thus well recognized, but hitherto suitable methods for this purpose have not been at hand. The situation in this respect for some time-independent properties is much better: For instance, methods such as the Diffusion Quantum Monte Carlo (DQMC) and related techniques have been used very effectively to compute ground-state energies and structural properties of large quantum clusters and solids.[15–18] Likewise, Feynman Path Integral methods were very successfully applied to the calculation of thermodynamic and structural properties of such systems at thermal equilibrium.[19–21] Another example are the ground and the low-lying vibrational eigenfunctions of large polyatomic molecules, that were recently calculated for several such systems by the Vibrational Self-Consistent

Field (VSCF) method and its extensions.[22–24] Thus, calculations of the ground and of the fundamental excited vib-rotational states were reported for the protein BPTI.[24]

Recently, the development of methods for time-dependent quantum simulations of large systems, was pursued vigorously by several research groups, and much progress was made. Some of the novel methods proposed are still confined to models or special systems, while for a few of the others realistic applications are already at hand. Examples of such recent methods are the Path Integral approach developed by Makri and coworkers[25,26] and the semiclassical centroid density approximation of Voth *et al.*[27,28]

The present article overviews two related recent methods for time-dependent quantum simulations of many-atom systems in which the present authors have been involved, the Time-Dependent Self-Consistent Field (TDSCF) and the Classically-Based Separable Potential (CSP) methods. While by no means developed to completion or general in applicability yet, these methods provide already practical working algorithms for a wide range of applications. Indeed, in the very short time since the introduction of the CSP method, many applications to large realistic systems were already made, showing that the method is already a "production tool" for extensive simulations. The TDSCF approximation is known, in the context of electronic structure theory, from the early years of quantum theory,[29] but its applications to problems of molecular dynamics are much more recent.[30–42,23] Methods of much improved accuracy were developed on the basis of the TDSCF approximation.[34–42] Also, some technical hurdles in applying the method for larger systems were overcome in the last few years at least for some types of interaction potentials, so recently calculations have been reported for problems of significantly increased number of degrees of freedom.[16,37] The second method we shall examine here for time-dependent quantum simulations of many-atom systems is the CSP approximation, and its generalizations.[43–48] This method, recently introduced by two of the present authors, has clearly been extensively applied to realistic systems, including problems where tens to hundreds of degrees of freedom are involved.[46] As in the case of TDSCF, much improved, more accurate approaches were built on the basis of the original, simple approximation.[48] At their simplest respective levels, both TDSCF and CSP involve approximations that separate the different modes, and treat each mode as moving in the average field of all the other modes. In TDSCF, the mean potentials that govern the different modes are computed quantum mechanically, by a self-consistent procedure. In CSP, the effective single-mode potentials are determined from independent classical Molecular Dynamics simulations carried out at the outset, and then used in the quantum calculation. In this paper the relative pros and cons of the TDSCF and CSP-based approaches will be analyzed, as will be the merits of these two methods with respect to other schemes that have been proposed for time-dependent quantum calculations for large systems. The applications that will be mentioned in the present paper, both for TDSCF and for CSP, are all for cluster systems. This seems to us a natural choice: In trying to develop simulation methods ultimately applicable to condensed phase problems, large clusters offer physical

properties similar to these phases, while still retaining the simplicity of finite systems.

Sec. 2 presents the TDSCF method and improved approaches built on it. Sec. 3 gives some examples of applications of TDSCF to the dynamics of clusters. Sec. 4 describes the CSP method and its extensions. Examples of applications of these methods to realistic clusters of many degrees of freedom are given in Sec. 5. The state-of-the-art for the two methods and directions for future progress and improvements are discussed in Sec. 6.

2 The Time-Dependent Self-Consistent Field (TDSCF) Approximation and its Extensions

2.1 TDSCF approximation

The TDSCF approximation, also known as the Time-Dependent Hartree (TDH) method dates from the early days of quantum theory.[29] The method was first introduced and used in electronic structure theory. In particular, a simplified (linearized), time-independent version of the method, known as the Random Phase Approximation was applied to electronic excited states of atoms and molecules, and in fact also to certain types of excited states encountered in nuclear physics.[49] Much later, the TDSCF was extensively used to study various nuclear collision processes.[50–53] Applications of the method to Quantum Molecular Dynamics simulations began in the 1980's, but were restricted until recently to systems of few degrees of freedom, special simple model potentials, etc.[31,54] Much more recently, technical difficulties were overcome and simulations of systems having up to ~ 40 degrees of freedom have already be reported.

To introduce the method, consider a molecular system of N degrees of freedom $q_1, ..., q_N$. The specific choice of the coordinates used is actually important for the TDSCF approximation, and we will later take up this point. The objective is to construct an algorithm for solving the time-dependent Schrödinger equation:

$$i\hbar\frac{\partial\Psi}{\partial t} = [-\sum_j \frac{\hbar^2}{2m_j}\frac{\partial^2}{\partial q_j^2} + V(q_1, ..., q_N)]\Psi \tag{1}$$

subject to an initial value $\Psi(q_1, ..., q_N, t = 0)$. Here m_j is the mass associated with coordinate j, and $V(q_1, ..., q_N)$ is the full potential function of the system. In the TDSCF approximation, a factorizable form is used for $\Psi(q_1, ...q_N, t)$:

$$\Psi(q_1, ..., q_N, t) = e^{i\gamma(t)}\prod_{j=1}^{N}\phi_j(q_j, t) \tag{2}$$

where the single-mode wavefunction $\phi_j(q_j,t)$ satisfies the Schrödinger equations:[23]

$$i\hbar\frac{\partial\phi_j(q_j,t)}{\partial t} = [-\frac{\hbar^2}{2m_j}\frac{\partial^2}{\partial q_j^2} + \bar{V}(q_j,t)]\phi_j(q_j,t) \tag{3}$$

and the effective single-mode potentials are given by:[23]

$$\bar{V}(q_j,t) = \langle\prod_{l\neq j}\phi_l(q_l,t)|V(q_1,...,q_N)|\prod_{l\neq j}\phi_l(q_l,t)\rangle \tag{4}$$

where the integrals (4) are over all $q_l, l \neq j$. The phase factor $e^{i\gamma(t)}$ is usually of no interest. In some cases, however, $\Psi(q_1,...,q_N,t)$ is used in equations for observables that are such that $\gamma(t)$ affects the results. For instance, the electronic absorption spectrum of a molecular system can be computed from the autocorrelation function of the wavefunction[14]. In calculations that employ this expression, the correct $\gamma(t)$ must be used. $\gamma(t)$ is given by:

$$\gamma(t) = \frac{1-N}{\hbar}\int_0^t \langle\prod_{j=1}^N\phi_j(q_j,t')|V(q_1,...,q_N)|\prod_{j=1}^N\phi_j(q_j,t')\rangle dt' \tag{5}$$

The TDSCF equations for the single-mode wavefunction $\phi_j(q_j,t)$ and effective potential $\bar{V}_j(q_j,t)$ are solved self-consistently for all the modes $j = 1,...,N$. To solve the single-mode Schrödinger equation (3), several suitable algorithms are available. The propagation method must, of course, be applicable for time-dependent potentials. Both Second-Order Differencing (SOD)[55] and the Feit-Fleck split-operator propagator[56] were extensively used. Of more recent methods that were suggested, the (t,t') algorithm[57] seems particularly advantageous for TDSCF. If the given initial state is factorizable, i.e.,

$$\Psi(q_1,...,q_N,t=0) = \prod_{j=1}^N\phi_j(q_j,t=0) \tag{6}$$

then an initial state for the propagation of each mode, $\phi_j(q_j,t=0)$ is readily available. However, in principle,. the TDSCF can be applied also in cases when the given initial state is non-separable. One can expand the initial state in a basis of separable states:

$$\Psi(q_1,...,q_N,t=0) = \sum_{\alpha=1}^{n_I}C_\alpha\prod_{j=1}^N\phi_j^{(\alpha)}(q_j,t=0) \tag{7}$$

For each separable basis state α, a TDSCF wavefunction is propagated from the initial single-mode states $\phi_j^{(\alpha)}(q_j,t=0)$, and the corresponding states $\phi_j^{(\alpha)}(q_j,t)$ are calculated in time. Thus, n_I separate TDSCF calculations are carried out, and in the end the approximate time-dependent wavefunction:

$$\Psi(q_1,...,q_N,t) = \sum_{\alpha=1}^{n_I}C_\alpha\prod_{j=1}^N\phi_j^{(\alpha)}(q_j,t) \tag{8}$$

Having outlined the TDSCF approximation, we now proceed to discuss its validity and accuracy, its scalability for large systems, and improved methods built on the TDSCF approximation.

2.2 Accuracy of TDSCF and the choice of coordinates

For systems where the dynamics may depend on the spin statistics of the atoms involved, the TDSCF *ansatz* (2) is clearly inadequate. This is pertinent to a limited class of systems, such as the weakly bound clusters of ^3He and ^4He. For such systems, a possible remedy is changing the Hartree-type *ansatz* (2) to a Hartree-Fock type *ansatz*, but this issue will not be treated here.

The *ansatz* of Eq. (2) is a separable one. Because of the time-dependence of the single-mode wavefunctions, the mean potential acting in each mode is time-dependent, and energy transfer between modes can take place within TDSCF. However, correlated motions of different modes are excluded by Eq. (2). The quality of the separability approximation depends obviously on the modes that are being separated. "Good modes" in the sense relevant to TDSCF are such that give rise to small correlation corrections only. There is no practical algorithm as yet for the determination of the optimal modes. Moreover, "good modes" in the above sense may not be convenient for practical calculations, especially for large systems. For instance, the problem of "good coordinates" arises also in *time-independent* SCF, which yields approximate vibrational eigenfunctions.[23] For rare-gas trimers, such as $Xe\ He_2$ and Ar_3, it was found that *hyperspherical coordinates* are excellent modes for SCF.[58,59] However, the kinetic energy expression in these modes is complicated, and they are not convenient for calculations. In practice, physical considerations have been the most important guide for choosing adequate coordinates, and the rapidly growing number of TDSCF applications shows that selecting reasonable coordinates in a given problem is not too difficult. A great deal of information on the accuracy of the TDSCF has come from comparison with exact results for small systems, including collinear triatomic systems, or realistic triatomic systems in 3D.[60–66] For instance, TDSCF was tested for vibrational predissociation of collinear models of van der Waals clusters[60] and for the same process in realistic 3D treatments of $I_2 - Ne$.[61] It was tested against exact calculations for photodissociation dynamics of HX molecules (X-halogen) in collinear models of Rg-HX [62] and also for photodissociation of HCl in Ar-HCl in full 3D.[63] TDSCF was studied and tested against exact calculations for transition-state dynamics in chemical reactions of the type X+HX in the framework of both collinear models and of realistic 3D systems.[64,65] In addition to the studies for small systems, TDSCF was also tested for a relatively large system such as $(Ar)_{13}$:[33] A TDSCF calculation was propagated for this system to (approximate) equilibrium in sufficiently long runs, and standard *equilibrium* properties were extracted from the results. The results were compared against Feynman Path Integral simulations of the same properties, which are "numerically exact".[33] Some of the insights that can be extracted from the various tests of TDSCF can be summarized as

follows:

(i) The accuracy of TDSCF is highest for short timescales, and generally decreases with increasing time. The fact that correlation effects build up in time is not surprising: In the course of a process, the wavepacket of a system generally breaks up, and as it keeps breaking up to more pieces, a separable wavefunction can no longer adequately describe the state. The important positive message is that for short timescales the TDSCF very often does very well: For photolysis of HX in Rg-HX clusters, the approximation is very accurate, at least to about 50 fs, which is a considerable timescale for this process.[62] It seems that typically for photochemical processes, TDSCF works very well, at least to the first 100 fs, and often to the picosecond timescale and longer - this with straightforward choices for the coordinates, which are unlikely to be "the last".

(ii) On the whole, the accuracy of TDSCF increases with the dimensionality of the system. TDSCF is similar in this respect to other "mean field" theories: The greater the number of degrees of freedom, the better become approaches based on averaging the potential acting on part of the system. For static SCF, strong evidence for such behavior was recently given.[67] Very interestingly, TD-SCF applied to the transition state dynamics of the Cl+HCl reaction was found much more accurate in the realistic 3D case, than for the collinear model of this system.[64] In fact, in the 3D case the approximation is almost exact for the transition state dynamics, while for the collinear system correlations between different modes are much stronger.

(iii) TDSCF is more accurate for coordinates such that there is a timescale separation between the different modes.[61,63,64] However, the method can work reasonably well even when the frequency separation between the modes is relatively modest.[65]

(iv) The TDSCF factorization of the full wavefunction into single-mode wavefunctions is only one version of the method. It is often possible to get much better accuracy by factorizing the total wavefunction into factors, each of which is a wavefunction of several modes.[61,63,64] Consider, for instance, the photodissociation of HCl in Ar-HCl. A TDSCF approach factorizing the wavefunction into a "hydrogenic" wavefunction and a "heavy atoms" wavefunction does better than TDSCF with full factorization to functions of single modes.[63]

(v) A specific but very important case where a satisfactory choice of "good coordinates" is available also for large systems: Low-energy excitations of a polyatomic system such that the dynamics remains confined to a limited vicinity of a single minimum of the potential surface. Normal modes are then an excellent choice for TDSCF.[33]

(vi) Processes such as chemical reactions cannot be described in a separable way from reagents to products by a single set of coordinates. Therefore, TDSCF fails in this case. (Note this does not apply to the limited aspect of transition state dynamics, where transition-state coordinates will do). A severe failure of TDSCF, at least when simple types of coordinates are used, can also occur for tunneling between two configurations of coupled-mode systems (since one set of modes may not be satisfactory for both configurations).[30,40] Substantial improvement or extension of TDSCF is required in these cases, and suitable

methods are indeed available for this, as will be discussed later.

2.3 Stability of TDSCF for large systems

For small systems where comparison with "numerically exact" methods can be made, TDSCF is computationally very efficient. In cases such as the photolysis of HCl in Ar-HCl or for the transition state dynamics of Cl+HCl (studied by electron photodetachment of $ClHCl^-$), TDSCF is by *more than an order of magnitude* more efficient than the corresponding exact calculation, while giving results of excellent quantitative accuracy.[64] Nevertheless, till very recently TDSCF was only applied to quite small systems. The difficulty in using the method for large systems lies in the evaluation of the average potentials $\bar{V}_j(q_j,t)$ of Eq. (4). In general this requires the calculation of multidimensional integrals, that must be carried out at every time step. In special cases this difficulty can be overcome essentially by simplifications of the potential surface.[33,67,68,69] and this is the basis for the progress made in applying TDSCF to larger systems. In general, the problem was still not overcome, and as we shall see later, as a consequence CSP is vastly superior to TDSCF in being scalable to much larger systems.

It was mentioned in the previous subsection that for low energy excitations in systems that are not extremely anharmonic, such that the dynamics is confined to the vicinity of a single minimum of the potential surface, normal modes are "good coordinates" for the accuracy of the TDSCF approximation. These coordinates can also be useful in such cases to greatly simplify the multidimensional integral problem of Eq. (4). Often, the potential function at the vicinity of the minimum to which the dynamics is confined can be expanded as a low-order polynomial in the normal modes:[33]

$$V(q_1,...,q_N) = \sum_{m_1,...,m_N} V_{m_1,...,m_N} (q_1)^{m-1} ... (q_N)^{m_N} \tag{9}$$

In this case only the evaluation of one-dimensional integrals is required to compute the effective potential $\bar{V}_j(q_j,t)$. The potentials are then given by:[67]

$$\bar{V}_j(q_j,t) = \sum_{m_1,...,m_N} V_{m_1,...,m_N} \prod_{l \neq j}^{N} F_{m_l}^{(l)}(t) (q_j)^{m_j} \tag{10}$$

where

$$F_{m_l}^{(l)} = \langle \phi_l(q_l,t) | (q_l)^{m_l} | \phi_l(q_l,t) \rangle \tag{11}$$

Although the number of one-dimensional integrals grows with the size of the system, if the order of the expansion is modest the computational task is feasible even for systems of hundreds of modes. This approach proved very successful in recent applications to systems such as $(Ne)_{13}$ and $(Ar)_{13}$.[33] It turns out that a quartic expansion of the potential is adequate for such cases. For very

anharmonic systems such as $(H_2O)_n$ clusters, this expansion fails for some of the modes, in particular for certain shearing and torsional modes,[67] though not for all the normal modes. Also for peptides, proteins and their complexes with water, which are very demanding in this respect, the normal modes expansion is at least valid for *most* modes (with adequate representation within the quartic level).[24]

Another case for which the mean potentials can be computed also for relatively large systems is when the potential can be written as a sum of pairwise mode-mode interactions only, in addition to single mode terms, i.e.,

$$V(q_1,...,q_N) = \sum_{j=1}^{N} V_j^{(S)}(q_j) + \sum_{j>i}^{N}\sum^{N} V_{ji}^{(P)}(q_j,q_i) \tag{12}$$

Such a form of the potential, in normal mode coordinates, proved very successful for clusters such as $(Ar)_{13}$,[67,68] $(H_2O)_n$,[67] and several others. In a recent study, representation (12) of the potential function was used for a TDSCF simulation of collision dynamics and energy transfer in $(Ar)_{13} + He$ scattering, in a full 3D framework.[68] Normal modes were employed in this study, and a grid method was used in evaluating the integratals for the mean-field potentials.[69] Many systems can be described by pair interactions between the *atoms*, but this can be useful in the present context only when the positions of the atoms are in themselves "good coordinates" for TDSCF, which is mostly not the case. The search for product representations of potential energy surfaces is being actively pursued, and progress was reported by Jackle and Meyer.[69] However, so far actual applications have been limited to few-atom systems.[69]

2.4 Extensions of TDSCF

Even in cases where the TDSCF approximation does well, it is important to have improvements of greater accuracy, preferably of a type that can in principle be pursued to the level of numerically exact results. The need for extensions is, of course, most critical for types of problems where TDSCF can break down completely or give poor results, as is often the case for chemical reactions,[70] tunneling in coupled-mode systems,[34,40,71] and in nonadiabatic processes.[72,73] Several approaches to improving the accuracy have been proposed. One of the interesting ideas has been to apply TDSCF in time-dependent coordinates, optimized so as to give good separability at every instant in time.[74] The method is, however, technically very cumbersome and was not hitherto applied to realistic cases. Another effort was to treat the difference between the exact Hamiltonian and the TDSCF one as a perturbation, and to employ time-dependent perturbation theory [(75)]. While the method worked well for simple model problems, it was not extended for realistic systems. It appears that the two most practical approaches for extending[34−40] TDSCF are the Multi-Configuration TDSCF (MC-TDCSF) and the Configuration Interaction TDSCF (CI-TDCSF).[41,42] The two methods are closely related. CI-TDCSF is simpler in the sense that the calculation of the single-mode wavefunction in this approach is easier and more

straightforward. On the other hand, MC-TDSCF is constructed to give single-mode wavefunctions that are in a variational sense optimal, as it may be the method of greater computational effectivity, especially for large systems. We describe here very briefly only MC-TDSCF, in the version of Meyer, Manthe and Cederbaum[36,37] who turned it into an effective and elegant algorithm. The MC-TDSCF *ansatz* for the wavefunction is:[36,37]

$$\Psi(q_1,...,q_N,t) = \sum_{j_1}^{n_1}...\sum_{j_f}^{n_N} a_{j_1...j_f}(t) \times \prod_{k=1}^{N} \phi_{j_k}^{(k)}(q_k,t) \tag{13}$$

To prevent redundant solutions, the following constraints are imposed on the single-mode wavefunctions:

$$\langle \phi_n^{(k)}(t) | \phi_m^{(k)}(t) \rangle = \delta_{nm} \tag{14}$$

$$\langle \phi_n^{(k)}(t) | \dot{\phi}_m^{(k)}(t) \rangle = \langle \phi_n^{(k)}(t) | - i h^{(k)} | \phi_m^{(k)}(t) \rangle \tag{15}$$

$h^{(k)}$ are single mode Hamiltonians that can be defined according to convenience. The full Hamiltonian is written as

$$H = \sum_{k=1}^{N} h^{(k)}(q_k) + U(q_1,...,q_N) \tag{16}$$

where the interaction U is nonseparable. The mean field interactions are defined by:

$$\langle U \rangle_{nm}^{(k)} = \langle \chi_n^{(k)} | U | \chi_m^{(k)} \rangle \tag{17}$$

The $\chi_n^{(k)}$ depend on all coordinates *except* q_k;

$$\chi_n^{(k)} = \sum_{all\ j_1,} ... \sum_{i \neq k} a_{j_1,...,j_{k-1},n,j_{k+1},...,j_N}(t) \times \prod_{l \neq k} \phi_{j_l}^{(l)}(q_l,t) \tag{18}$$

From a time-dependent variational principle and from the above relations one arrives at the following equations of motion for the coefficients $a_J(t)$, which represent a global notation for the corresponding coefficients in Eq. (13):

$$i\hbar \dot{a}_J(t) = \sum_L \langle \Phi_J | U | \Phi_L \rangle a_L(t) \tag{19}$$

Here J and L are collective indices ($J = j_1...j_N$), and

$$\Phi_J = \prod_{l=1}^{N} \phi_{j_l}^{(l)}(q_l) \tag{20}$$

The equation of motion obeyed by the single-mode wavefunction is, in vector notation

$$i\hbar \dot{\phi}^{(k)} = h^{(k)} \phi^{(k)} + [1 - P^{(k)}] \rho^{(k)-1} \langle \mathbf{U} \rangle^{(k)} \phi^{(k)} \tag{21}$$

here $\phi^{(k)}$ is a vector of single-mode wavefunctions, $\rho^{(k)}$ - density matrix constructed from the wavefunction $\chi_n^{(k)}$ of (17), and $P^{(k)}$ is a time-dependent projection on the space spanned by the single-mode wavefunction $\phi_j^{(k)}$. $\langle U \rangle^{(k)}$ are the matrix representations of the mean field interactions defined in (17). The MC-TDSCF calculation consists of propagating single-mode wavefunctions and coefficients of configurations (given by eq. (20)) in time, according to (19), (21). The method can be of very high accuracy. However, it has mostly been applied to small systems. A recent application by Worth *et al.*,[37] for the absorption spectrum of Pyrazine includes all 24 vibrational modes of this molecule, but is for a very simple model Hamiltonian. In our view, MC-TDSCF is a "high-end" approximation that expands significantly the scope of the available "numerically exact" approaches in being able to deal reliably with systems of more degrees of freedom than the latter methods could. It is still not, in the present state-of-the-art, a simulation method for very large systems.

3 Applications of TDSCF

The TDSCF method, and its extensions such as MC-TDSCF, have been extensively applied to systems of a few atoms.[36,38,39,42,61,64,65,69] We give here only examples of applications to relatively large, realistic systems, which in fact are hitherto rather few.[33,37,68,77] Two topics will be discussed: Applications to inelastic scattering in collisions of large clusters with atoms[68,77] and application to simulations of equilibrium states of rare gas clusters.[33]

3.1 TDSCF calculations of atom collisions with clusters

Calculations of inelastic and reactive scattering processes are one of the outstanding challenges to quantum molecular dynamics. Of particular importance are, for example, the calculations of state-to-state transition probabilities, or of the survival probabilities of the given quantum initial state in the collision. Such quantities cannot be classically computed, except through the use of crude "quantization" procedures, which box assign the continuous classical scattering distributions into "boxes" representing quantum states. Methods such as TDSCF and CSP are paving the way for quantum calculations of large-system collision dynamics. Two such calculations, in which several of the present authors were involved, were recently carried out: Collisions of He with $(Ar)_{13}$ clusters,[68] and collisions of Ar atoms with $(H_2O)_{11}$ clusters.[77] In both calculations, all modes of the cluster were included, as both calculated transition probabilities (and cross sections) into final quantum states. Modeling of the initial states corresponding to realistic conditions, require inclusion of all possible initial orientations of the cluster (as implied by the $J = 0, m_J = 0$ initial quantum rotational state that was assumed), and of all collision impact parameters. Thus, different TDSCF calculations were carried out for several impact parameters, providing a sufficient sampling of this variable, and likewise with

respect to the orientation in space of the cluster with respect to the collision axis. In both studies the TDSCF treatment was not applied to the colliding atom, which was described classically only. This approximate treatment of the collider was used because the focal aspect in the two studies was on the internal vibrational states of the cluster, and on the importance of quantum effects pertinent to these states. Extension of the TDSCF treatment to include quantum description of the collision partner, while implying an increase of the computational effort, is feasible, and is indeed being pursued in current calculations. The TDSCF calculations on $Ar + (H_2O)_{11}$ were carried out in a semiclassical framework, describing each mode by semiclassical Gaussian wavepackets,[78] while $(Ar)_{13} + He$ was described by full quantum TDSCF. There is approximately a factor of 5 in cpu favoring the semiclassical TDSCF calculation over the quantum TDSCF for systems of this type. A simplified representation of the full potential function, along the lines discussed in Sec. (II.c) was employed in both cases. Both studies[68,77] considered clusters initially at their vibrational ground state, and collisions at low energies, which involve modes energy transfer only into the internal modes. For such cases, normal coordinates are expected to be good for the TDSCF approximation, as noted in Sec. (II.c). In the study on $He + (Ar)_{13}$, the potential function was represented by single-mode terms and by pairwise-mode interactions, found to be very adequate for this system.[68] In the case of $Ar + (H_2O)_{11}$, the potential function was expanded up to quartic terms in the normal modes.[77] For small $(H_2O)_n$ clusters ($n < 5$, say) such a treatment may involve significant errors due to the very large anharmonicity of the systems.[67] For larger clusters such as $(H_2O)_{11}$, the system is "stiff" enough to justify the expansion. In fact, for the above two systems it seems that two simplifications for the potential discussed here both seem to work well.

Fig. 1 and Fig. 2 show results from the TDSCF simulation of $Ar+(H_2O)_{11}$ collisions. The collision energy used was 0.09 eV and, as mentioned above, the cluster was initially at the vib-rotational ground state. Fig. 1 shows the mean excitation energy for each (normal) mode, as a function of mode number. (The modes are ordered in decreasing stiffness. The lowest modes numbers correspond essentially to the stiff intramolecular stretching vibrations of the H_2O monomers within the cluster, while the large mode numbers corresponds to collective vibrations and soft torsional and shearing modes). The TDSCF results are compared with classical Molecular Dynamics results. Since the modes are not really completely separable, the residual interaction energies were divided between the modes, but the effect of this approximate treatment was tested and found small. As Fig. 1 shows, the classical results deviate quite considerably from the TDSCF ones. The main error of the classical calculation is that also many stiff modes undergo excitation quite effectively, although quantum mechanically such processes are forbidden since the energy transferred is less than the (quantum) gap between the ground state and the fundamental excited state for that transition. The fact that classical dynamics can transfer arbitrarily small amounts of energy into a given mode of excitation, since it does not include the aspect of energy quantization of the target system, is of large quantitative importance in this example. Fig. 2 gives the excitation

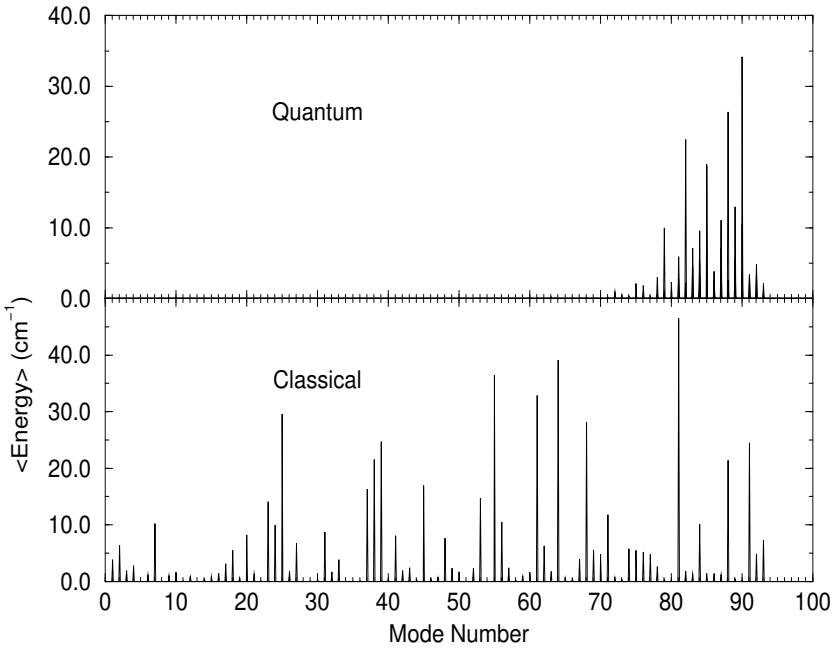

Figure 1: Mean excitation energy for each mode in Ar+$(H_2O)_{11}$ collisions

probability of the initial state with respect to the different modes of excitation. This probability $P_{ex}(n)$ is the sum of excitation probabilities into all final states n of that mode, except $n = 0$. The TDSCF results are compared to classical results, to which crude "box quantization" of the final mode energy was applied - the classical energy was histogrammed into boxes. Again, the "box-quantized" classical results deviate greatly from the TDSCF. It seems that the "box quantization" condition counts too many events as "non-excitations". The two figures, 1 and 2, show how important are the quantum effects for such systems in low-energy collisions, *when state-specific information is required*. In conclusion of this type of application we mention findings from the $He + (Ar)_{13}$ simulation, that seem of general interest. First, it was found that there are specific state-to-state transitions for this system that are of observable magnitude. This may be surprising since the number of possible final states in this system, even at the low collision energy used, is very large and one may have expected a statistical "dilution", rendering any specific final state of too small a magnitude to be observed. In fact, there are a few specific transitions for that system having a cross section of about 10 $\AA^2$. The excitation process is thus highly non-statistical. All the important excitations in this case are of the type

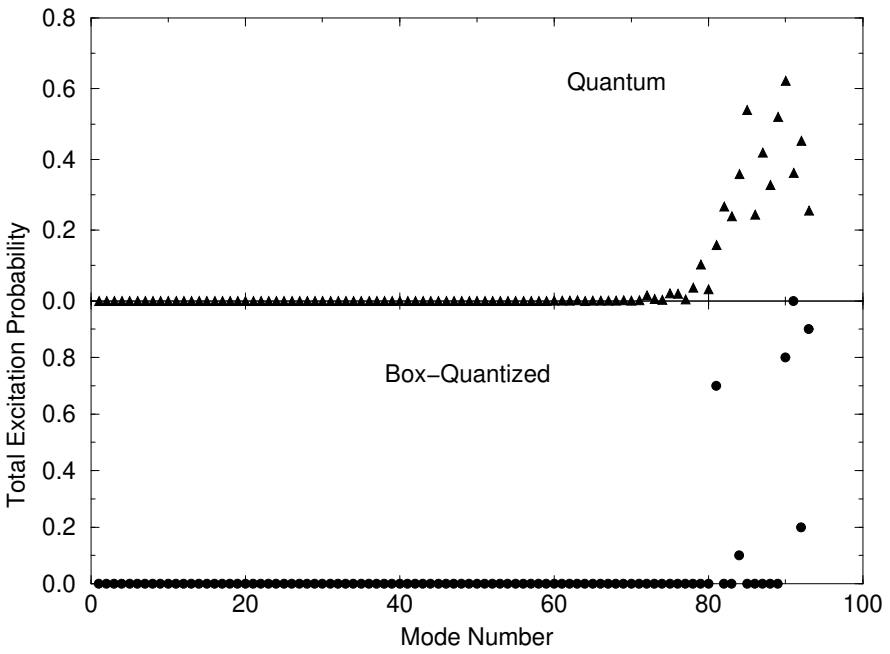

Figure 2: Total probability of undergoing excitation versus mode number in $Ar+(H_2O)_{11}$ collisions

$\nu_j = n_1 = 0, ..., n_{33} = 0 \rightarrow \nu_f = n_1 = 0, ..., n_j, ..., n_{33} = 0$, where n_j is either 1 or 2, i.e., along single "phonon" or two "phonon" excitations important. In fact, some of the two quantum excitations are as important as the single-quantum ones.

3.2 Application of TDSCF to simulation of clusters at equilibrium

One of the main uses of classical MD simulations is for the description of equilibrium properties of systems.[79] The algorithms for this purpose propagate a trajectory for a selected value of the total energy but otherwise essentially arbitrary initial conditions. After sufficient time of propagation, assuming the system is ergodic, equilibration will set in. Taking snapshots of the system at random time points after equilibration, can yield an ensemble that represents the equilibrium configurations of the system.[79] It is very desirable to develop such a tool also for quantum MD simulations. In a recent study it was shown that this can be done in the framework of TDSCF, at least in certain cases.[33] The simulations were carried out for $(Ne)_{13}, (Ar)_{13}$, and used semiclassical TDSCF,

with Gaussian single-mode wavefunctions. The following procedure was used: A (Gaussian) TDSCF wavefunction was propagated from an initial state of suitable energy expectation value, but otherwise arbitrary (i.e., the position of the center of the Gaussian in configuration space, the initial momenta of the modes and the widths of the single modes of the Gaussians are all chosen quite arbitrarily, subject to the desirable energy expectation value only). The TDSCF equations are propagated for several picoseconds, which for the systems studied was sufficient for (approximate) equilibration. The system is then sampled at random time points t_j, and an ensemble of Gaussian wavepackets

$$G_j(\mathbf{q}) = G(q_1, ..., q_N, t_j) \tag{22}$$

is obtained, where $G(\mathbf{q}, t)$ is the propagated semiclassical TDSCF wavepacket. Only linearly independent $G_j(\mathbf{q})$ are accepted, in fact approximate orthogonality

$$\langle G_j | G_k \rangle \approx 0 \qquad \text{if} \qquad j \neq k \tag{23}$$

is used as an acceptance condition. The process is converged when the set of G_j can span any other wavefunction of the same expectation value. The set of the $G_j(\mathbf{q})$ is equivalent to the (equilibrium) density matrix of the system. The above procedure is for a "mirocanonical" distribution. To obtain a thermal ensemble at temperature T, one uses a set of initial states, each of which is propagated as above, and with the states such that their expectation values sample the Boltzmann distribution.[33] Since the Feynman Path Integral (FPI) method[19] is available for structural equilibrium properties, it can be used to test the TDSCF simulations. Fig. 3 shows the Ar-Ar pair distance distribution of $(Ar)_{13}$ at $T = 5K$. The TDSCF results are compared with the numerically exact FPI and the agreement is excellent. The classical MD results are shown for comparison. The classical distribution is narrower, basically because the classical results do not contain the zero-point amplitudes. While the FPI is numerically exact, the TDSCF simulations have the advantage that they can also be used to study dynamical properties (such as frequencies) at equilibrium, and also the equilibration dynamics itself. Also for other important properties, e.g. Wigner phase space momentum-position distribution, the use of the TDSCF is computationally far more convenient than that of FPI.

4 The Classically-Based Separable Potential (CSP) Method and Its Extensions

The general idea behind the CSP approach is to use input from Classical Molecular Dynamics simulations, carried out for the process of interest as a first preliminary step, in order to simplify a quantum mechanical calculation, implemented in a subsequent, second step. This takes advantage of the fact that classical dynamics offers a reasonable description of many properties of molecular systems, in particular of average quantities. More specifically, the method uses classical

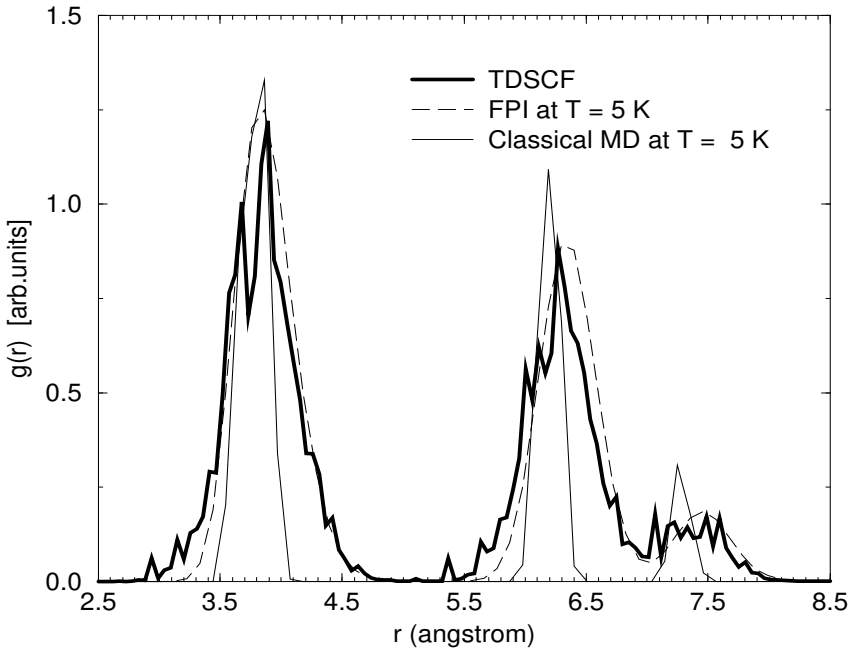

Figure 3: Ar-Ar distance distribution in $(Ar)_{13}$

MD simulations in order to determine effective potentials such that by the use of the latter a subsequent quantum calculation becomes far simpler[43)−(48)].

4.1 The CSP approximation

We give here a brief outline of the methods as introduced in Refs. 43, 44, and 47. Suppose that the initial state of the system is $\psi_0(q_1, ..., q_N)$. From ψ_0, the Wigner phase-space distribution $D(q_1, ..., q_N; p_1, ..., p_N)$ is computed. This distribution is used to sample initial positions and momenta $q_1^{(\alpha)}, ..., q_N^{(\alpha)}; p_1^{(\alpha)}, ..., p_N^{(\alpha)}$, for a classical trajectory simulation of the process of interest. The set of trajectories $q_1^{(\alpha)}(t), ..., q_N^{(\alpha)}(t)$, for $\alpha = 1, ..., n_T$, can be used to generate in the classical framework any quantity of interest at each time point t. From the trajectories, we compute the average potential acting on each mode j:

$$\bar{V}_j(q_j, t) = \sum_{\alpha=1}^{n_T} V(q_1^{(\alpha)}(t), ..., q_{j-1}^{(\alpha)}(t), q_j, q_{j+1}^{(\alpha)}(t), ..., q_N^{(\alpha)}(t))\omega_\alpha + \frac{1-N}{N}\bar{V}(t) \quad (24)$$

where $V(q_1, ..., q_N)$ is the full potential function of the system, and the summa-

tion in (24) extends over all MD trajectories. ω_α is the weight of the α trajectory in the initial state distribution (as determined from the Wigner distribution). Note that in (24), all the coordinates q_l are evaluated at trajectory points, except the q_j for which the mean potential $\bar{V}_j(q_j,t)$ is evaluated. The j-th coordinate is kept as in the full potential function. $\bar{V}(t)$ in (24) is a coordinate-independent function of time given by:

$$\bar{V}(t) = \sum_{\alpha=1}^{n_T} V(q_1^{(\alpha)}(t), ..., q_j^{(\alpha)}(t), ..., q_N^{(\alpha)}(t))\omega_\alpha \tag{25}$$

The inclusion of the second term on the right-hand-side of (24) is convenient, because in this way the average (over the trajectories) of the sum of the single-mode potentials, $\sum_{j=1}^{n} \bar{V}(q_j,t)$, equals to the average of the full potential function $V(q_1,...,q_N)$. Using the single-mode effective potentials $\bar{V}_j(q_j,t)$, one can solve a time-dependent Schrödinger equation for each mode:

$$i\hbar \frac{\partial \phi_j(q_j,t)}{\partial t} = [T_j + \bar{V}_j(q_j,t)]\phi_j(q_j,t) \tag{26}$$

where T_j is the kinetic energy operator for mode j. A separable approximation for the total wavepacket of the system is given by

$$\psi(q_1,...,q_N,t) = \prod_{j=1}^{N} \phi_j(q_j,t) \tag{27}$$

With the above definitions, there is no additional overall phase factor to be included in (27). Eqs. (24)-(27) are the CSP approximation.[43–47] Like TDSCF, CSP is a separable approximation, using a time-dependent mean potential for each degree of freedom. However, the effective potentials in CSP are obtained from classical MD, and their evaluation is computationally very easy, not involving multidimensional integrals as in the case of TDSCF. This gives CSP a computational advantage that for large systems is enormous, especially for systems where the potential function cannot be simplified to reduce the dimensionality of the TDSCF integrals.

4.2 Accuracy of the CSP approximation

The accuracy of the CSP approximation is, as test calculations for model systems show, typically very similar to that of the TDSCF.[43] The reason for this is that for atomic scale masses, the classical mean potentials are very similar to the quantum mechanical ones. CSP may deviate significantly from TDSCF in cases where, e.g., the dynamics is strongly influenced by classically forbidden regions of phase space. However, for simple tunneling cases it seems not hard to "fix" CSP, by running the classical trajectories slightly above the barrier. In any case, for typical systems the classical estimate for the mean potential functions works extremely well.

It should be noted that due to the use of classical trajectories to evaluate the time-dependent single-mode potentials, the quantum CSP energy is not strictly conserved (TDSCF conserves energy, since the single-mode potentials are obtained self-consistently with the single-mode wavefunctions). The extent of the non-conservation is, however, small and it does not seem to create significant difficulties. The smaller the difference between the TDSCF and the CSP single-mode potentials, the smaller is the CSP energy non-conservation. The more near-classical a system is, the smaller is the non-conservation effect. In general, CSP is expected to be less accurate than TDSCF, although only slightly so, because the quantum effects are not included in the evaluation of the single-mode potentials. In special cases, however, CSP may give slightly better results than TDSCF, because the CSP mean-potentials are calculated from an approach that includes correlation effects between the modes (classical MD). In summary: TDSCF and CSP give very similar results in most cases, but for systems with appreciable quantum effects, TDSCF is more accurate than CSP, while the latter may prove somewhat accurate when correlation effects are quite important.

It is obvious that CSP depends, as does TDSCF, on the choice of coordinates. As pointed out in Sec. 2.2, numerical convenience often limits the choice of the coordinates. CSP may, however, offer practical prospects for the choice of physically optimal modes. The deviation of the true potential from CSP separability is given by:

$$\Delta V_{corr}(q_1, ..., q_N, t) \equiv V(q_1, ..., q_N) - \sum_{j=1}^{N} \bar{V}_j(q_j, t) \tag{28}$$

ΔV_{corr} can be evaluated readily from the classical MD simulation for any choice of coordinate system, and it may be possible to determine the modes that give the smallest ΔV_{corr}. These should be optimal CSP modes. Work along these lines is in progress in our group. So far, however, the coordinate choices in the CSP applications were all straightforward and based on qualitative physical consideration.

4.3 Extensions of CSP

The main extension hitherto introduced for the CSP approximation is referred to as the Configuration Interaction CSP (CI-CSP) method.[48] This approach represents the full non-separable wavepacket as a linear combination, with time-dependent coefficients, of terms that are each separable. The applications of this method are very encouraging. The method can provide major improvements over CSP, and can probably be pursued at a level of high accuracy, while still being computationally feasible for large systems.[48] The method is flexible, and allows for the use of physical considerations to optimize it. The most important advantage is that within CI-CSP, the classical MD simulations greatly simplify the determination of the terms or configurations, that play the

most important role in the total wavefunction. The approach is based on the following: The CSP wavepacket is obtained from mean single-mode potentials, computed as an average over all the trajectories. To include correlation effects, it is necessary to include also wavefunction terms computed from potentials that represent "fluctuations" from the average. Such potentials can be computed along a limited set of trajectories, even individual trajectories (rather than as an average over all trajectories). In the version of CI-CSP discussed here, we start with propagating separable wavepackets using effective potentials obtained from individual trajectories:

$$\bar{V}_j^{(\alpha)}(q_j,t) = V(q_1^{(\alpha)}(t),...,q_{j-1}^{(\alpha)}(t),q_j,q_{j+1}^{(\alpha)}(t),...,q_N^{(\alpha)}(t)) + \frac{1-N}{N}\bar{V}^{(\alpha)}(t) \quad (29)$$

The coordinate-independent quantities $\bar{V}^{(\alpha)}(t)$ are given by:

$$\bar{V}^{(\alpha)}(t) = V(q_1^{(\alpha)},...,q_j^{(\alpha)}(t),...,q_N^{(\alpha)}(t)) \quad (30)$$

In addition to wavepackets propagated along effective potentials corresponding to individual trajectories, we also propagate in CI-CSP the CSP wavefunctions, governed by the average potentials $\bar{V}_j(q_j,t)$ of Eq. (24). The CI-CSP *ansatz* for the total wavepacket of the system is then as follows:[48]

$$\Psi(q_1,...,q_N,t) = c_o(t)\prod_{j=1}^{N}\phi_j(q_j,t) + \sum_{j,\alpha}^{N,M_j} s_j^{(\alpha)}(t)\phi_1...\phi_j^{(\alpha)}...\phi_N +$$

$$+ \sum_{j<j',\alpha,\beta}^{N,M_j,N,M} d_{j\alpha j'\beta}(t)\phi_1...\phi_j^{(\alpha)}...\phi_{j'}^{(\beta)}...\phi_N \quad (31)$$

Here $\phi_j(q_j,t)$ are the CSP functions, $\phi_j^{(\alpha)}(q_j,t)$ denotes the q_j-mode wavefunction propagated on the effective potential generated from the α trajectory. These wavefunctions are orthogonalized and included in the CI expansion when the overlap between ϕ_j and $\phi_j^{(\alpha)}$ drops below a certain threshold (typically 99%). In this way, the CI space grows in the course of the dynamical evolution, corresponding to the increase of correlation between the modes. In the above expansion, M_j is the number of trajectories actually included in the CI expansion (with respect to functions of the mode j), $c_o(t)$ is the CSP coefficient, $s_j^{\alpha}(t)$ are single mode excitation coefficients, while $d_{j\alpha j'\beta}(t)$ are coefficients corresponding to two-mode excitations. The language of excitation is borrowed from time-independent CI in electronic structure theory,[80] with which the present formulation has strong analogies. Within this analogy, the *ansatz* (31) corresponds to configuration interaction with single and double excitations (neglecting higher-order excitations). From a physical point of view one should rather talk about mode-mode correlations instead of double excitations and mode 'polarization' terms instead of single excitations but we stay with the usual notation. To obtain equations of motion for the coefficients $c_o(t), s_j^{\alpha}(t), d_{j\alpha j'\beta}(t)$ of the wavefunction

expression (31), we substitute the *ansatz* into the time-dependent Schrödinger equation of the system, Eq. (1), with the fully coupled potential. To get practical working equations we make several approximations:

(i) Consider for simplicity the case when the initial state is separable (extension to a non-separable initial state is straightforward, though technically more complicated). Then at $t = 0, c_o = 1$ and all the other CI coefficients are zero. In a short-time approximation we then take into account only coupling between the CSP state, and doubly excited states (it can be shown that coupling between CSP and singly excited states is always zero - this is a time-dependent analogue of the Brillouin theorem, familiar from electronic structure theory[80]). In this way we neglect very small (at least initially) single-single, single-double, and double-double excitation couplings.

(ii) Consider an integral $\langle\Phi|V|\hat{\Phi}\rangle$ where Φ and $\hat{\Phi}$ differ in two modes j and $j\prime$ only. We approximate this integral by $\langle\phi_j\phi_{j\prime}|V^{CSP2}_{jj\prime}|\hat{\phi}_j\hat{\phi}_{j\prime}\rangle$, where

$$V^{CSP2}_{jj\prime}(q_j, q_{j\prime}, t) = \sum_{\alpha=1}^{n_T} V(q_1^{(\alpha)}(t), ..., q_j, ..., q_{j\prime}, ..., q_N^{(\alpha)}(t))\omega_\alpha \tag{32}$$

where n_T is the total number of trajectories.

Substitution of the *ansatz* (31) into the Schrödinger equation (1) for the full system, together with the above approximations, yields the following equations for the coefficients $c_o(t), d_{j\alpha j\prime\beta}(t)$ of the CI expansion (31):

$$i\frac{\partial c_o}{\partial t} = \sum_{j,\alpha,j\prime,\beta}^{N,M,N_j,M_{j\prime}} d_{j\alpha j\prime\beta}(t)\langle\phi_j\phi_{j\prime}|V^{CSP2}_{jj\prime}|\hat{\phi}_j^{(\alpha)}\hat{\phi}_{j\prime}^{(\beta)}\rangle \tag{33}$$

$$i\frac{\partial d_{j\alpha j\prime\beta}(t)}{\partial t} = c_o(t)\langle\hat{\phi}_j^{(\alpha)}\hat{\phi}_{j\prime}^{(\beta)}|V^{CSP2}_{jj\prime}|\phi_j\phi_{j\prime}\rangle \tag{34}$$

For separable initial states the "single excitation" terms can be set to zero at all times at this level of approximation. Eqs. (32),(33),(34) together with the CSP equations and with the *ansatz* (31) for the total wavefunction are the working equations for the approach. This form, without further extension, is valid only for short time-domains (typically, a few picoseconds at most). For large times, higher correlations, i.e. interactions between different singly and doubly excited states must be included.

4.4 Comments on computational implementation of CSP and CI-CSP

A very important computational advantage of CSP and CI-CSP for large systems is that the methods can be applied to any potential function without any need to simplify the latter by expansion, assumption of pairwise interactions, etc., as is the case for TDSCF. Applications of CSP for systems having up to $\sim 10^3$ degrees of freedom, and of CI-CSP for systems of up to ~ 100 modes

are not computationally extremely demanding, and were indeed carried out on quite modest scalar workstations, of the type of SGI Indigo, HP Appollo, etc. Finally, implementation of CSP on a parallel computer is straightforward, and almost ideal in efficiency. Indeed, in recent work in our group, CSP was already implemented on MOSIX, a computer of distributed architecture, developed by Professor A. Barak (Hebrew University). A high degree of parallelization efficiency was obtained. We anticipate shortly CSP applications on computers such as MOSIX for systems having over 10^4 degrees of freedom, and such calculations for biological molecules are currently under way in our group. The high degree of parallelization stems, of course, from the fact that each degree of freedom within CSP is formally autonomous, with its own effective potential and without self-consistency requirements etc. that can be a complication. Some parallelization of CI-CSP is also possible, although this was not yet carried out.

5 Applications of CSP and of CI-CSP

Computational efficiency is a major advantage of CSP and CI-CSP. Almost from the introduction of these methods, applications to large systems with realistic potential functions became possible. A "canned" CSP code was written and is available.[47] The applications of CSP so far include a study of electron photodetachment dynamics for $I^-(Ar)_{12}$,[44] a study of the dynamics following electronic excitation of $Ba(Ar)_n$ for $n = 10$, $n = 20$,[45] and a study of electronic excitation, cage effects and vibrational dephasing and relaxation dynamis for I_2 in $I_2(Rg)_n$, for $Rg = Ar$, Xe and $n = 17, 47$ (corresponding respectively to complete first and complete first two solvation layers around the iodine).[47] The dynamics of $Ba(Ar)_n$ following the excitation of the Ba in this cluster involves nonadiabatic transitions, since there are three quasidegenerate p-states of the Ba atom, and the system is then governed by three potential energy surfaces corresponding to these state, with possible non-adiabatic transitions between them. The simulations of Ref. 45 thus went beyond simple CSP, and were in fact a three-configuration CI-CSP, with a separable term in the CI wavefunction for each adiabatic electronic state. This approach, while not a converged quantum treatment, is expected already to be more reliable than semiclassical "surface hopping" methods that treat nuclear motions classically.[81] Comparison of the CI-CSP with semiclassical "surface hopping" simulations for $Ba(Ar)_{10}$ and $Ba(Ar)_{20}$, suggests that the "surface hopping" results for properties such as population ratios of the electronic states at, say, $t \approx 1$ ps after excitation, can differ from quantum results by a significant factor, of the order of ~ 2 in this case.[45]

For $I_2(Ar)_{17}$, an extensive CI-CSP simulation was carried out,[48] and the results were compared with those of the simple CSP approximation.[46] Both calculations are for the ultrafast dynamics following excitation of the I_2 into the B state. We found that the CI-CSP calculation, including "doubly excited configurations", is close to converged for times up to $t \sim 500$ fs, when 1500 configurations are included. Fig. 4 shows $|c_o(t)|^2$, the coefficient of the CSP

term and the doubly excited terms $|d_{j\alpha j\prime\beta}|^2$ in the full CI-CSP wavefunction, versus time.

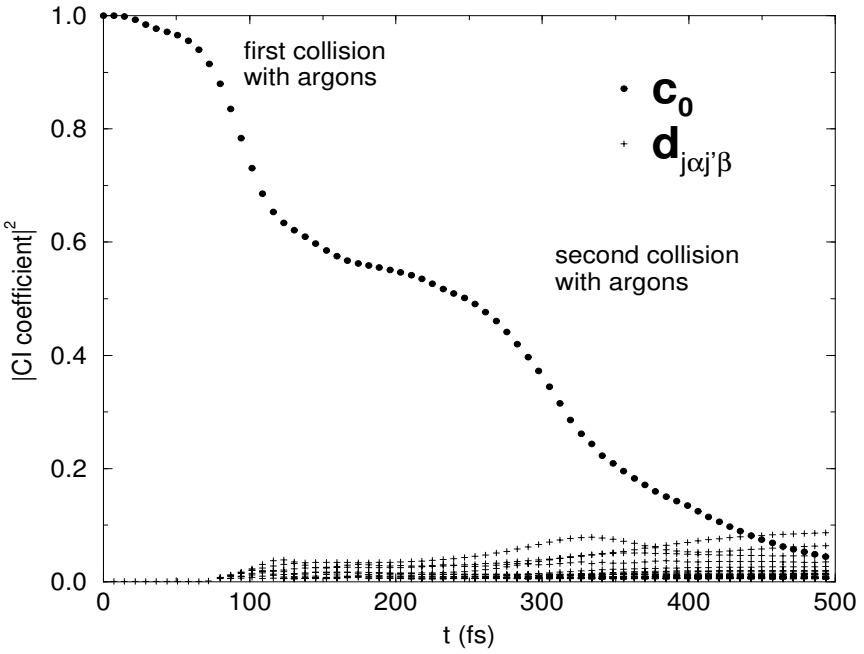

Figure 4: The contribution c_o of the CSP approximation to the CI wavefunction and the correlation coefficients $d_{j\alpha j\prime\beta}$ versus time.

It turns out that the CSP approximation dominates the full wavefunction, and is therefore almost exact till $t \approx 80$ fs. This timescale is already very useful: The first ≈ 20 fs are sufficient to determine the photoadsorption lineshape and, as turns out, the first ≈ 80 fs are sufficient to determine the Resonance Raman spectrum of the system. Simple CSP is almost exact for these properties. As Fig. 4 shows, for later times the accuracy of the CSP decays quickly: for $t \approx 500$ fs in this system, the contribution of the CSP approximation to the full CI wavefunction is almost negligible. In addition, this wavefunction is dominated not by a few specific terms of the CI expansion, but by a whole host of configurations. The "decay" of the CSP approximation was found to be due to "hard collisions" between the iodine atoms and the "surrounding wall" of argons. Already the first hard collision brings a major deterioration of the CSP approximation, but also the role of the second collision can be clearly identified. As was mentioned, for $t < 80$ fs, the CSP is essentially of quantitative accuracy. Fig. 5 shows the Resonance Raman spectrum for $I_2(Ar)_{17}$.[46]

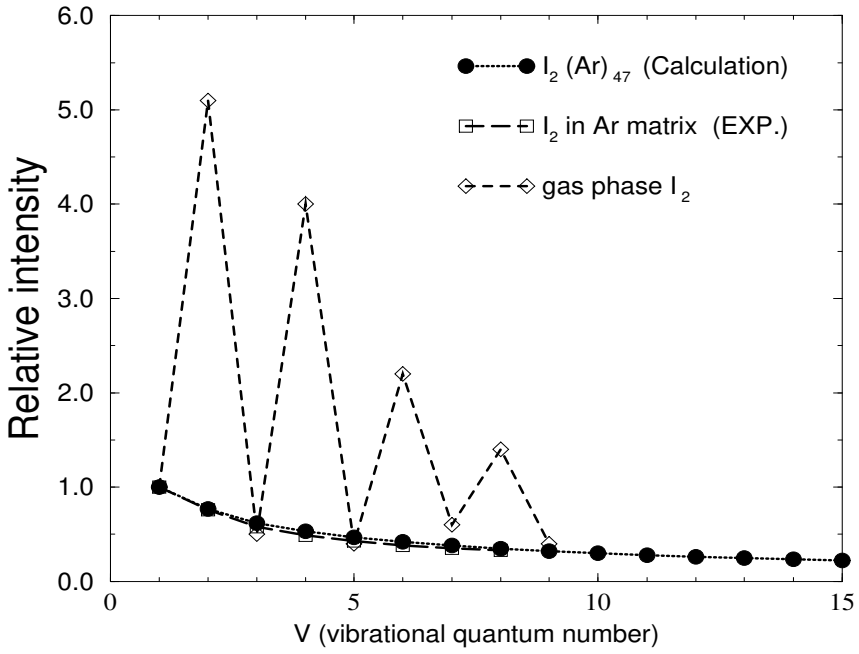

Figure 5: Resonance Raman Intensities for I_2 $(Ar)_{47}$

The intensities are plotted vs. v, the final vibrational quantum number of the transition. The CSP results (which for this property are almost identical with CI-CSP) are compared with experimental results for I_2 in a low-temperature Ar matrix.[82] The agreement is excellent. Also shown is the comparison with gas-phase, isolated I_2. The "solvent effect" on the Raman intensities is clearly very large and qualitative. These show that CSP calculations for short timescales can be extremely useful, although for later times the method breaks down, and CI-CSP should be used.

6 Concluding Remarks

In this article we discussed and examined two methods for time-dependent quantum simulations of many-atom systems: The TDSCF-based and the CSP-based algorithms. Both of these methods begin, at their simplest level, with a separable approximation for the wavefunction, and describe each mode as governed by a mean time-dependent potential due to the other modes. The CSP approach determines the effective potentials from classical MD simulations, while in TDSCF, they are determined by a self-consistent quantum-mechanical procedure.

Both methods can and have already been applied to systems of substantial sizes, and are thus already practical simulation tools. CSP and its extensions, by using classical MD to simplify the effective Hamiltonian and thus the subsequent quantum-mechanical part of the simulation, are far superior to TDSCF in computational efficiency for large systems, and especially in scalability to very large systems. Applications of CSP and CI-CSP to systems having of the order of ~ 100 degrees of freedom are already at hand, and CSP calculations for biomolecules of 10^4 degrees of freedom are in advanced stages of progress. Applications to TDSCF for larger systems depend on the possibility of certain simplifications of the potential functions, which is a considerable restriction. On the other hand, for the smaller range of systems TDSCF is usually somewhat more accurate than CSP, and this is especially the case when there are very strong quantum effects. For those smaller systems, MC-TDSCF, which can be carried out to a very high degree of accuracy, is probably superior in that respect to CI-CSP. For both methods, the introduction of correlation effects between modes is computationally the most demanding aspect of the approach. In our belief, a search for simplified methods for correlation corrections should be one of the most useful directions to be followed in the future. An efficient treatment of important correlation effects will benefit in particular processes involving, e.g., chemical (substitution) reactions and nonadiabatic processes, in which the role of dynamical correlations is both extremely important and hard to handle computationally.

We expect that in the forthcoming few years CSP-based and TDSCF-based methods will be extensively used as practical tools of application for an increased range of processes, and at the same time the search for methodological improvements will continue towards a universally applicable tool, flexible and computationally more effective Quantum Molecular Dynamics.

Acknowledgement

We thank Joon O. Jung and Dr. S. Gregurick for helpful discussions and suggestions. We also thank Professor M.A. Ratner, Professor R.D. Coalson, Dr. U. Manthe and Dr. Alison Marks for helpful comments. Some of the calculations discussed here were carried out on the MOSIX parallel computer system of Professor A. Barak (Computer Sciences, Hebrew University). We thank Professor Barak for his help, and the Ministry of Science, State of Israel, for a grant (to R.B.G.) that supported this research. Calculations discussed here were also carried out on the SP2 computer of the Inter-University Computing Center, Israel. This work was also supported by a grant from the Ministry of Science, Israel (to R.B.G.). Research described here was also supported under the auspices of the Louis P. and Saerree K. Fiedler Chair in Chemistry (held by R.B.G.).

Part of the research described here was carried out at U.C. Irvine, and supported by the Chemistry Division of the NSF (grant CHE-9503258 to R.B.G.). P.J. and R.B.G. were supported by an international US NSF - Czech Government grant No. 445944-21210/ES010.

7 References

1. G.C. Schatz, *J. Phys. Chem.* **100**, 12839 (1996).

2. R. Kosloff, *Ann. Rev. Phys. Chem.* **45**, 145 (1994).

3. J.Z.H. Zang and W.H. Miller, *J. Chem. Phys.* **92**, 1811 (1990).

4. U. Manthe, T. Seideman and W.H. Miller, *J. Chem. Phys.* **92**, 10078 (1990).

5. D. Neuhauser, *J. Chem. Phys.* **9272** (1994).

6. U. Peskin and N. Moiseyev, *J. Chem. Phys.* **99**, 4590 (1993).

7. D.J. Kouri, Y. Houng, W. Zhu and D.K. Hoffman, *J. Chem. Phys.* **100**, 3362 (1994).

8. D.H. Zang and J.Z.K. Zang, *J. Chem. Phys.* **100**, 2679 (1994).

9. R. Schinke, *Photodissociation Dynamics* (Cambridge University Press, Cambridge, 1993).

10. W.H. Miller, *Adv. Chem. Phys.* **30**, 77 (1975).

11. E.J. Heller, *J. Chem. Phys.* **94**, 2723 (1994).

12. B.W. Spath and W.H. Miller, *J. Chem. Phys.* **104**, 95 (1996).

13. J.G. Kay and W.H. Miller, *J. Chem. Phys.* **104**, 95 (1996).

14. G.C. Schatz and M.A. Ratner, *Quantum Mechanics in Chemistry* (Prentice Hall, New Jersey, 1993).

15. J.B. Anderson, *J. Chem. Phys.* **63**, 1499 (1975).

16. M.A. Suhm and R.O. Watts, *Phys. Rep.* **204**, 293 (1991).

17. M.A. McMahan, R.N. Barnet and K.B. Whaley, *J. Chem. Phys.* **99**, 8816 (1993).

18. S. Broude and R.B. Gerber, *Chem. Phys. Lett.* **258**, 416 (1996).

19. D. Scharf, G.J. Martyna and M.L. Klein, *J. Chem. Phys.* **99**, 8997 (1993).

20. V. Buch, *J. Chem. Phys.* **100**, 7610 (1994).

21. D. Scharf, G.J. Martyna, D. Li, G.A. Voth and M.L. Klein, *J. Chem. Phys.* **99**, 9013 (1993).

22. J.M. Bowman, *Acc. Chem. Res.* **19**, 202 (1986).

23. R.B. Gerber and M.A. Ratner, *Adv. Chem. Phys.* **70**, 97 (1988).

24. A.E. Roitberg, R.B. Gerber, R. Elber and M.A. Ratner, *Science* **268**, 1319 (1995).

25. N. Makri, *Chem. Phys. Lett.* **193**, 435 (1992).25. N. Makri, *Chem. Phys. Lett.* **193**, 435 (1992).

26. M. Topaler and N. Makri, *Chem. Phys. Lett.* **210**, 285 (1993).

27. J. Cao and G.A. Voth, *J. Chem. Phys.* **100**, 5106 (1994).

28. J. Cao and G.A. Voth, *J. Chem. Phys.* **101**, 6168 (1994).

29. P.A.M. Dirac, *Proc. Camb. Phil. Soc.* **26**, 376 (1930).

30. E.J. Heller, *J. Chem. Phys.* **64**, 63 (1976).

31. R.B. Gerber, V. Buch and M.A. Ratner, *J. Chem. Phys.* **77**, 3022 (1982).

32. Z. Li and R.B. Gerber, *J. Chem. Phys.* **99**, 8637 (1993).

33. E. Fredj, R.B. Gerber and M.A. Ratner, *J. Chem. Phys.* **105**, 1121 (1996).

34. N. Makri and W.H. Miller, *J. Chem. Phys.* **87**, 5781 (1987).

35. H.-D. Meyer, U. Manthe and L.S. Cederbaum, *Chem. Phys. Lett.* **165**, 73 (1990).

36. U. Manthe, H.-D. Mayer and L.S. Cederbaum, *J. Chem. Phys.* **97**, 3199 (1992).

37. G.A. Worth, H.-D. Mayer and L.S. Cederbaum, *J. Chem. Phys.* (in press).

38. J.-Y. Fang and H. Guo, *J. Chem. Phys.* **101**, 5831 (1994).

39. J.-Y. Fang and H. Guo, *J. Chem. Phys.* **102**, 2404 (1995).

40. Z. Kotler, E. Neria and A. Nitzan, *Comput. Phys. Commun.* **63**, 243 (1991).

41. J. Campos-Martinez and R.D. Coalson, *J. Chem. Phys.* **93**, 4740 (1990).

42. A.D. Hammerich, R. Kosloff and M.A. Ranter, *Chem. Phys. Lett.* **171**, 97 (1990).

43. P. Jungwirth and R.B. Gerber, *J. Chem. Phys.* **102**, 6046 (1995).

44. P. Jungwirth and R.B. Gerber, *J. Chem. Phys.* **102**, 8855 (1995).

45. P. Jungwirth and R.B. Gerber, *J. Chem. Phys.* **104**, 5803 (1996).

46. P. Jungwirth, E. Fredj and R.B. Gerber, *J. Chem. Phys.* **104**, 9932 (1996).

47. P. Jungwirth, E. Fredj, P. Zdanska and R.B. Gerber, *J. Comput. Chem.* (submitted).

48. P. Jungwirth, E. Fredj and R.B. Gerber (to be published).

49. D.J. Thouless, *The Quantum Mechanics of Many-Body Systems* (Academic Press, New York, 1961) pp. 88-93.

50. P. Bonche, S.E. Koonin and J.W. Negele, *Phys. Rev.* **C13**, 1226 (1976).

51. S. Lent, *Phys. Rev.* **C21**, 1594 (1980).

52. J.W. Negele, *Physics Today* **38**, 24 (1985).

53. K. Goeke and P.-G. Reinhard, *Time-Dependent Hartree-Fock and Beyond*, Lecture Notes in Physics, Vol. 171 (Springer-Verlag, Berlin, 1982).

54. V. Buch, M.A. Ratner and R.B. Gerber, *Chem. Phys. Lett.* **101**, 44 (1983).

55. R.B. Gerber, R. Kosloff and M. Berman, *Comput. Phys. Reports* **5**, 59 (1986).

56. M.D. Feit, J.A. Fleck and A. Steiger, *J. Comp. Phys.* **47**, 412 (1982).

57. U. Peskin, R. Kosloff and N. Moiseyev, *J. Chem. Phys.* **99**, 4590 (1993).

58. T.R. Horn, R.B. Gerber and M.A. Ratner, *J. Chem. Phys.* **91**, 1813 (1989).

59. T.R. Horn, R.B. Gerber, J.J. Valentini and M.A. Ratner, *J. Chem. Phys.* **94**, 6728 (1991).

60. R.H. Bisseling, R. Kosloff, R.B. Gerber, M.A. Ratner, L. Gibson and C. Cerjan, *J. Chem. Phys.* **87**, 2760 (1987).

61. A. Garcia-Vela, *J. Chem. Phys.* **104**, 1047 (1996).

62. R. Alimi, R.B. Gerber, A.D. Hammerich, R. Kosloff and M.A. Ratner, *J. Chem. Phys.* **93**, 6484 (1990).

63. A. Garcia-Vela and R.B. Gerber, *J. Chem. Phys.* **103**, 3463 (1995).

64. A.B. McCoy, R.B. Gerber and M.A. Ratner, *J. Chem. Phys.* **101**, 1975 (1994).

65. A.B. McCoy, *Mol. Phys.* **85**, 965 (1995).

66. Z. Li and R.B. Gerber, *Chem. Phys. Lett.* **104**, 5803 (1996).

67. J.O. Jung and R.B. Gerber, *J. Chem. Phys.* (in press).

68. A.Y. Rom and R.B. Gerber, *J. Chem. Phys.* (submitted).

69. A. Jäckle and H.-D. Meyer, *J. Chem. Phys.* **104**, 7974 (1996).

70. A. Jäckle and H.-D. Meyer, *J. Chem. Phys.* **102**, 5605 (1995).

71. G.D. Billing and G. Jolicard, *Chem. Phys. Lett.* **221**, 75 (1994).

72. J.R. Waldeck, J. Campos-Martinez and R.D. Coalson, *J. Chem. Phys.* **94**, 2773 (1991).

73. N.P. Blake and H. Metiu, in *Femtosecond Chemistry*, ed. J. Manz and L. Wöste (VCH, Weinheim, 1995) p. 532.

74. J. Kucar, H.-D. Meyer and L.S. Cederbaum, *Chem. Phys. Lett.* **140**, 525 (1987).

75. R.B. Gerber and A. Alimi, *Chem. Phys. Lett.* **184**, 69 (1991).

76. J. Campos-Martinez and R.D. Coalson, *J. Chem. Phys.* **99**, 9629 (1993).

77. E. Fredj, R.B. Gerber and M.A. Ratner (to be published).

78. E.J. Heller, *J. Chem. Phys.* **62**, 1544 (1975).

79. M.P. Allen and D.J. Tildesley, *Computer Simulation of Liquids*, (Clarendon, Oxford, 1987).

80. R. McWeeny, *Methods of Molecular Quantum Mechanics*, 2nd edition (Academic Press, San Diego, 1992).

81. A.I. Krylov, R.B. Gerber, M.A. Gaveau, J.M. Mestdagh, B. Schilling and J.P. Visticot, *J. Chem. Phys.* **104**, 3651 (1996).

82. J.F. Grzykowski and L. Andrews, *J. Raman Spectros.* **4**, 99 (1975).